# The Cyclin-Dependent Kinase Inhibitor Orysa;KRP1 Plays an Important Role in Seed Development of Rice[1][W]

**Rosa Maria Barrôco[2], Adrian Peres[2,3], Anne-Marie Droual[2], Lieven De Veylder, Le Son Long Nguyen, Joris De Wolf, Vladimir Mironov, Rindert Peerbolte, Gerrit T.S. Beemster, Dirk Inzé*, Willem F. Broekaert, and Valerie Frankard**

Department of Plant Systems Biology, Flanders Interuniversity Institute for Biotechnology, Ghent University, B–9052 Ghent, Belgium (R.M.B., L.D.V., L.S.L.N., V.M., G.T.S.B., D.I.); and CropDesign NV, B–9052 Ghent, Belgium (A.P., A.-M.D., J.D.W., R.P., W.F.B., V.F.)

Kip-related proteins (KRPs) play a major role in the regulation of the plant cell cycle. We report the identification of five putative rice (*Oryza sativa*) proteins that share characteristic motifs with previously described plant KRPs. To investigate the function of KRPs in rice development, we generated transgenic plants overexpressing the Orysa;*KRP1* gene. Phenotypic analysis revealed that overexpressed *KRP1* reduced cell production during leaf development. The reduced cell production in the leaf meristem was partly compensated by an increased cell size, demonstrating the existence of a compensatory mechanism in monocot species by which growth rate is less reduced than cell production, through cell expansion. Furthermore, Orysa;*KRP1* overexpression dramatically reduced seed filling. Sectioning through the overexpressed *KRP1* seeds showed that KRP overproduction disturbed the production of endosperm cells. The decrease in the number of fully formed seeds was accompanied by a drop in the endoreduplication of endosperm cells, pointing toward a role of KRP1 in connecting endocycle with endosperm development. Also, spatial and temporal transcript detection in developing seeds suggests that Orysa;KRP1 plays an important role in the exit from the mitotic cell cycle during rice grain formation.

Cell division is controlled by the activity of cyclin (CYC)-dependent kinase (CDK) complexes. In addition to their association with CYCs, the activity of CDKs is also regulated by other mechanisms, including activation of CDKs through phosphorylation of Thr-161 by a CDK-activating kinase, inactivation of the CDK/CYC complex via phosphorylation of the Thr-14 and Tyr-15 residues by WEE1 kinase, and degradation of CYC subunits (for review, see De Veylder et al., 2003; Dewitte and Murray, 2003; Inzé, 2005). A further level of regulation of CDK activity involves the so-called CDK inhibitors (CKIs).

CKI proteins directly inhibit CDK activity by binding to the CDK/CYC complexes (Sherr and Roberts, 1999; Lui et al., 2000). In mammals, two families of CKIs have been identified: the INK4 and the Kip/Cip, including $p21^{Cip1}$, $p27^{Kip1}$, and $p57^{Kip2}$. The INK4 inhibitors ($p16^{INK4A}$, $p15^{INK4B}$, $p18^{INK4C}$, and $p19^{INK4D}$) only bind the G1-specific CDK complexes, CDK4 and CDK6, and are characterized by the presence of four or five ankyrin repeats. To date, no plant counterparts of INK4 inhibitors have been identified. The Kip/Cip proteins bind to a wide range of CDK complexes, with a preference for G1- and S-phase complexes (Sherr and Roberts, 1995). All mammalian Kip/Cip inhibitors have a common amino-terminal domain involved in binding to both CDKs and CYCs.

In plants, all the CKI proteins that have been identified share a limited similarity to the mammalian $p27^{Kip1}$ inhibitor. Therefore, plant CKIs are designated Kip-related proteins (KRPs; De Veylder et al., 2001), but also as interactors of CDC2 kinases (ICKs; Wang et al., 1997). In contrast to the mammalian inhibitors, the conserved CDK/CYC-binding domain is located at the C-terminal side of the protein. In tobacco (*Nicotiana tabacum*), a KRP-like inhibitor designated NtKIS1a was isolated by a yeast two-hybrid screen. Overexpression of this gene in Arabidopsis (*Arabidopsis thaliana*) reduced CDK kinase activity (Jasinski et al., 2002).

[1] This work was supported in part by a grant from the Institute for the Promotion of Innovation by Science and Technology in Flanders (TraitQuest grant no. 000391 and postdoctoral fellowship to R.M.B.), the European Research Training Network (DAGOLIGN project HPRN–CT–2002–00267 [fellowship to A.P.] and Marie Curie Industry Host Fellowship Horyzan project HPMI–CT–1999–00056 [fellowship to A.-M.D.]), and the Research Foundation-Flanders (postdoctoral fellowship to L.D.V.).

[2] These authors contributed equally to the paper.

[3] Present address: European Commission, Joint Research Centre, Institute for Reference Materials and Measurements, B–2440 Geel, Belgium.

* Corresponding author; e-mail dirk.inze@psb.ugent.be; fax 32–9–3313809.

The author responsible for distribution of materials integral to the findings presented in this article in accordance with the policy described in the Instructions for Authors (www.plantphysiol.org) is: Valerie Frankard (valerie.frankard@cropdesign.com).

[W] The online version of this article contains Web-only data.
www.plantphysiol.org/cgi/doi/10.1104/pp.106.087056

Also, the tomato (*Lycopersicon esculentum*) LeKRP1 has recently been shown to inhibit CDK/CYC kinase activities in endoreduplicating cells of the gel tissue (Bisbis et al., 2006). In Arabidopsis, seven ICK/KRP proteins (KRP1–KRP7) have been identified through yeast two-hybrid and in silico screenings (for review, see Verkest et al., 2005b). Because all Arabidopsis ICK/KRP proteins bind and inhibit exclusively CDKA;1 and not with B-type CDKs, they might arrest the cell cycle both at the G1/S and G2/M boundaries in response to specific developmental or environmental cues. Abscisic acid and cold induce *ICK1/KRP1* expression and decrease CDK-mediated histone H1 kinase activity (Wang et al., 1998), whereas *ICK2/KRP2* expression is negatively regulated by auxin during early lateral root initiation (Himanen et al., 2002).

Targeted expression of the Arabidopsis *ICK1/KRP1* was obtained with the trichome-specific *GL2* (Schnittger et al., 2003) and floral organ-specific *AP3* promoters of Arabidopsis, and the *Bgp1* pollen-specific promoter of rape (*Brassica napus*; Zhou et al., 2002b). The transgenic plants appeared morphologically normal, but the development of the organs in which the ICK1/KRP1 protein was ectopically overproduced was strongly inhibited. Moreover, Arabidopsis trichomes overexpressing *ICK1/KRP1* initiated a cell death program, demonstrating a link between *ICK1/KRP1* expression and programmed death (Schnittger et al., 2003).

Additionally, transgenic plants have been generated that overexpress *KRP* genes by means of a constitutive promoter (Wang et al., 2000; De Veylder et al., 2001; Jasinski et al., 2002; Zhou et al., 2002a). In all cases, drastic developmental abnormalities were reported, such as overall reduced growth evidenced by smaller/shorter vegetative and reproductive organs. Morphological deviations were also observed, such as strong leaf serration and enlarged cells. Detailed analyses showed that increased *KRP* expression resulted in reduced CDK activity and decreased endoreduplication. Besides their role in cell proliferation and in cell cycle exit, plant KRPs have an important function in tuning the mitosis-to-endocycle transition (Verkest et al., 2005a; Weinl et al., 2005).

In monocotyledonous plants, the structural and functional characteristics of KRPs are largely unknown. Recently, Coelho et al. (2005) reported the characterization of two maize (*Zea mays*) genes, Zeama;*KRP1* and Zeama;*KRP2*, which are expressed during endosperm development. The encoded proteins were shown to inhibit plant CDK activity, and Zeama;KRP1 was proposed to play a role in the endoreduplication process during endosperm formation (Coelho et al., 2005).

Here, we report the identification of rice (*Oryza sativa*) *KRP* genes and the functional characterization of one of these. The phenotype of transgenic *KRP1*-overexpressing ($KRP1^{OE}$) rice plants suggests the importance of KRPs for plant growth as well as a prominent role in seed development.

## RESULTS

### Identification of Rice *KRP* Genes and Characterization of Orysa;*KRP1*

To search for rice KRP members, we screened the rice genomic database for proteins containing highly conserved plant KRP hallmarks (GRYEW and KYNFD; De Veylder et al., 2001). Five putative rice KRPs were identified, hereafter designated Orysa;*KRP1* to Orysa;*KRP5* (Fig. 1A). It should be noted that the proteins were numbered sequentially and, consequently, that the KRP members from rice and other species should not be regarded as systematic orthologs. Sequence similarity between the KRPs of rice and other plants is mostly concentrated in a region of 40 amino acids located at the extreme C-terminal end of each KRP, which encompasses the conserved motifs 1, 2, and 3 of plant ICK/KRPs (De Veylder et al., 2001; Jasinski et al., 2002). Conserved motifs 1 and 2 include the CDK-binding box, whereas motif 3 corresponds to the CYCD-binding box (Wang et al., 1998).

Sequences of rice KRP1, KRP2, and KRP3 comprise nuclear localization signals (Fig. 1A), whereas KRP2 (amino acids 160–176) and KRP4 (amino acids 126–138) have a putative PEST domain. These two functional domains have been detected in some other plant KRPs as well (De Veylder et al., 2001; Jasinski et al., 2002).

By phylogenetic analysis of plant KRPs, rice KRPs were found to form two groups: KRP1 is more closely related to KRP2 and KRP3, whereas KRP4 and KRP5 cluster in a separate group (Fig. 1B). Sequence analysis suggests that Orysa;KRP1 and Orysa;KRP2 are the two most closely related rice KRPs, sharing 51% identity at the amino acid level. Orysa;KRP4 shares high amino acid similarity to Zeama;KRP1, whereas Zeama;KRP2 clusters with Orysa;KRP2 and Orysa;KRP3. Overall, the phylogenetic analysis supports a separation of monocot KRPs into two different groups, whereas that between dicot members is less obvious.

### Generation of Orysa;*KRP1*-Overexpressing Lines

For this study, we chose to characterize KRP1 in more detail. First, its sequence was verified by sequencing a full-length cDNA clone that was isolated from a rice cell suspension cDNA library using a PCR-amplified probe corresponding to a partial Orysa;*KRP1* cDNA sequence. To investigate the possible role of Orysa;KRP1 in rice development, we generated transgenic plants overexpressing the gene under the control of the constitutive rice *GOS2* promoter (de Pater et al., 1992). Quantitative evaluation of transcript levels following transformation showed that the Orysa;*KRP1* gene was overexpressed in all four independent transformation events analyzed (Supplemental Fig. S1). Expression levels were increased for all tissues analyzed (roots, shoots, and leaves).

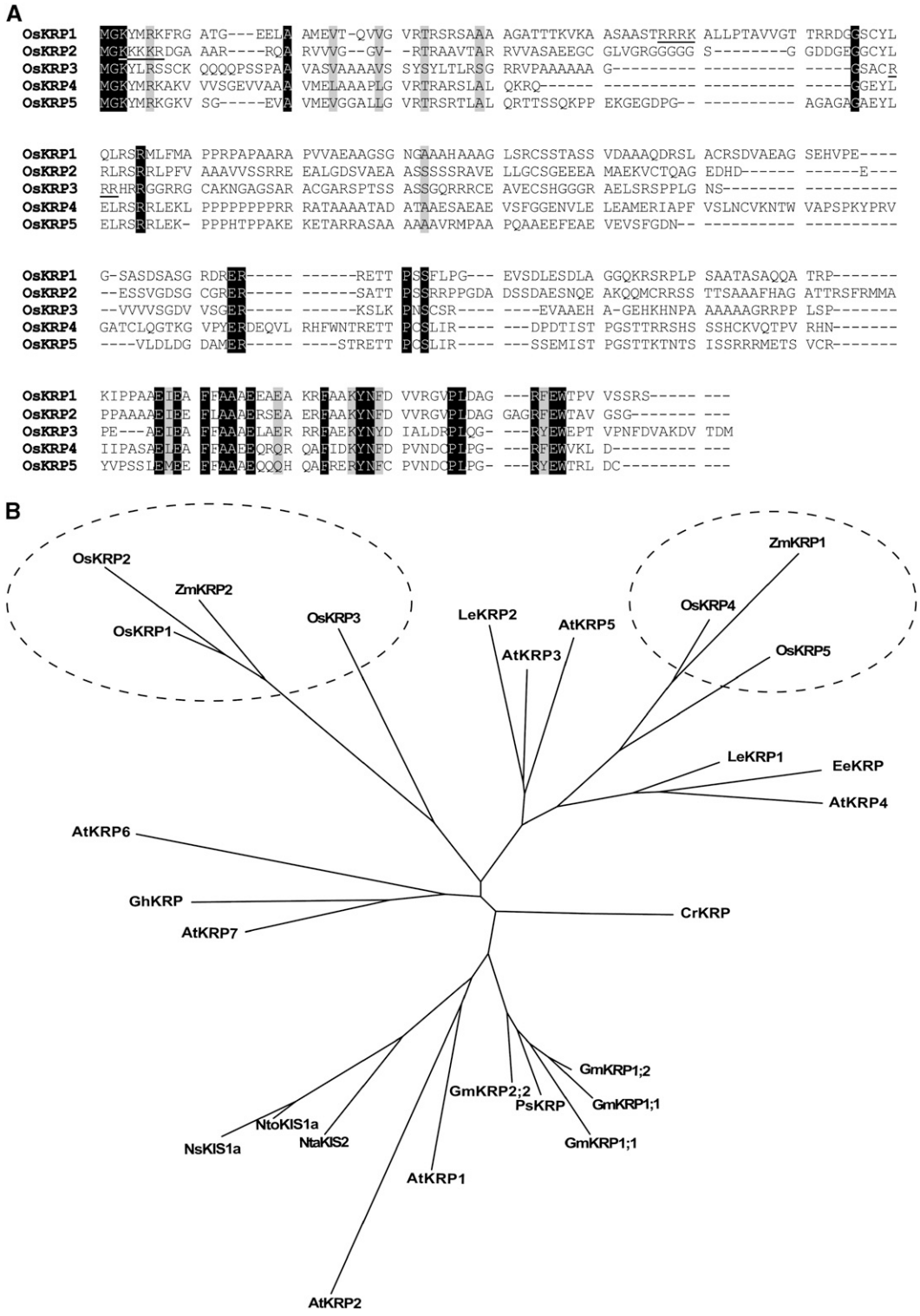


**Figure 1.** Analysis of the amino acid sequences of rice KRPs. A, Amino acid sequence alignment of the predicted KRPs from rice. Identical and conserved amino acids are indicated by dark gray and light gray shading, respectively. Putative nuclear localization signals are underlined. B, Neighbor-joining tree of the C-terminal conserved region of plant KRPs, illustrating the relationship among these proteins. The tree branches including rice KRPs are circled. For simplification, the species names are designated by the first letters of the genus and species names. At, *A. thaliana*; Cr, *Chenopodium rubrum*; Ee, *Euphorbia esula*; Gh, *Gossypium hirsutum*; Gm, *Glycine max*; Le, *L. esculentum*; Ns, *Nicotiana sylvestris*; Nta, *N. tabacum*; Nto, *Nicotiana tomentosiformis*; Os, *O. sativa*; Ps, *Pisum sativum*; Zm, *Z. mays*.

### *KRP1* Overexpression Inhibits Leaf Growth

The vegetative growth of the rice plants overexpressing *KRP1* was investigated. Total vegetative growth of the *KRP1*$^{OE}$ plants was recorded by digital image analysis on a weekly basis. The transgenic plants had slightly smaller leaf areas and were shorter than the controls in three out of the four lines analyzed, but the differences were not significant at a *P* value of 0.05 (Fig. 2A; Supplemental Table S1). Also, the time to reach 90% of the maximal aboveground plant area did not vary statistically for the transgenic and control plants.

Although no major differences were observed in the vegetative growth of the entire plant, ruler measurements showed that leaf elongation rates (LERs) of the sixth leaf from overexpressing plants were at least 20% slower than those of control leaves ($P < 0.05$). Maximum LER of transgenic plants was 0.26 cm $h^{-1}$, whereas the control plants grew at 0.33 cm $h^{-1}$ (Fig. 2E). The duration of the leaf elongation period was unaffected by the transgene and so the final leaf length was decreased by nearly 14% in the overexpressing plants (Fig. 2D; $P < 0.05$). To further understand the cellular basis of reduced leaf growth rates, mature epidermal cell lengths were measured. As observed in Figure 2, B and C, epidermal cells of *KRP1*$^{OE}$ leaves were significantly larger than those of control plants (93.7 $\mu$m versus 78.6 $\mu$m; Fig. 2F), indicating that the lower LERs in transgenic plants might be due to reduced cell production, which is partly offset by increased cell expansion. Indeed, cell production was severely reduced in transgenic plants. During the first 56 h following leaf emergence, overexpressing plants produced per cell file 26.1 cells $h^{-1}$ versus 39.6 cells $h^{-1}$ for the control (Fig. 2G; $P < 0.05$). In summary, the overexpression of *KRP1* in rice strongly decreases cell number in leaves, but total leaf growth is only moderately affected because of compensation by increased cell size. In contrast, the transgene had no significant effect on growth rate or cell size of the primary root

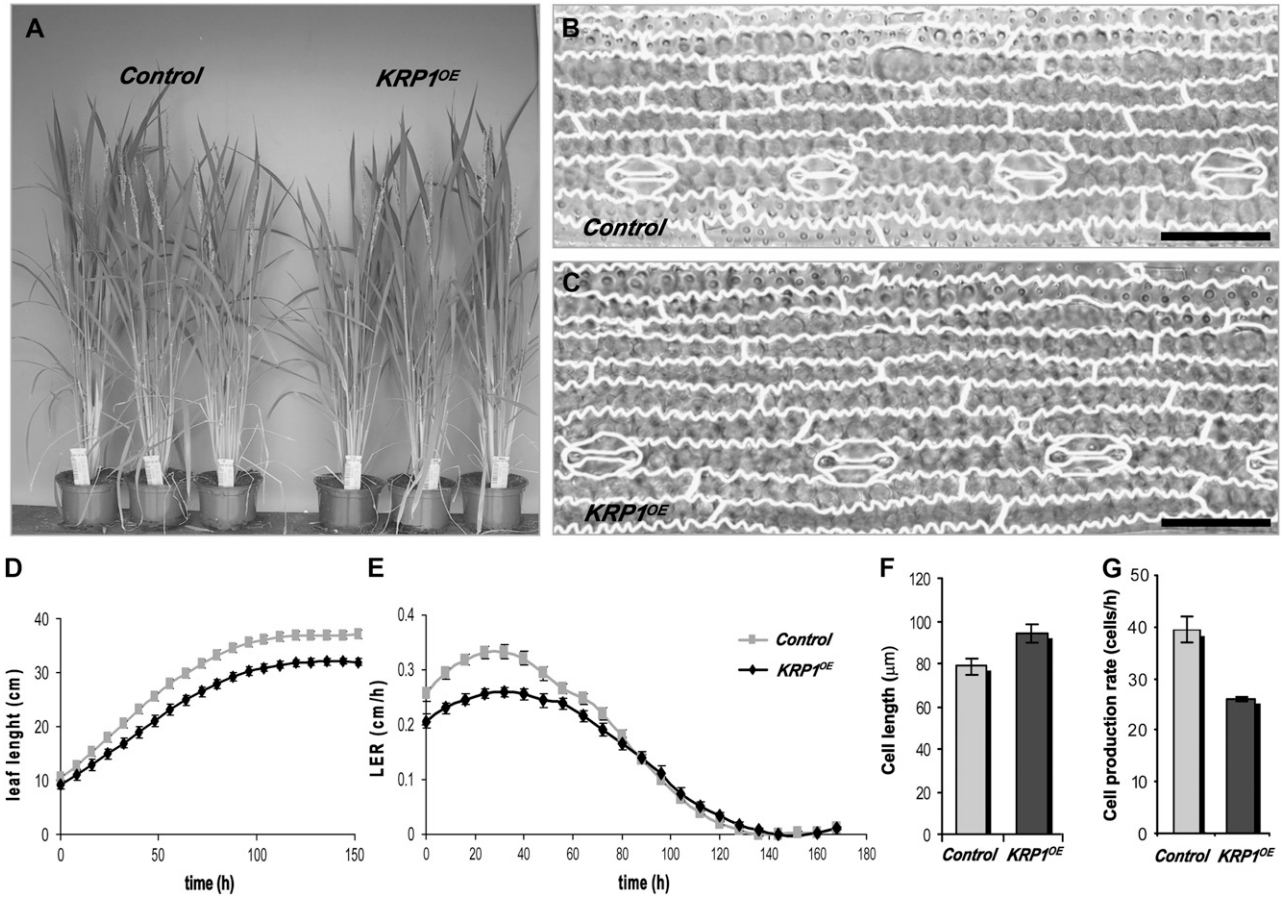


**Figure 2.** Phenotypic analysis of Orysa;*KRP1*-overexpressing leaves. A, Flowering *KRP1*$^{OE}$ plants (right) and corresponding controls (left). B and C, Epidermal cells of the mature regions of the sixth leaf from control and *KRP1*$^{OE}$ plants, respectively. In both images, cell walls were highlighted by a white pencil to make the cell boundaries more clearly visible. Bar = 50 $\mu$m. D, Growth curves of the sixth leaf of *KRP1*$^{OE}$ (black) and control plants (gray). E, LERs of transgenic *KRP1*$^{OE}$ and corresponding control plants. Error bars represent SE ($n = 15$). F, Mature cell length of *KRP1*$^{OE}$ and control leaves ($n = 100$). G, Rates of cell production per meristematic cell file of *KRP1*$^{OE}$ (black) and control (gray) leaves ($n = 15$).

(data not shown), indicating insensitivity of this organ to the presence of the transgene.

### *KRP1* Overexpression Alters Rice Seed Production

Phenotypic evaluation of transgenic Orysa;*KRP1*$^{OE}$ plants revealed striking differences in seed production when compared to the corresponding controls. Seed production was significantly reduced in the $T_1$ transgenic plants of all four lines analyzed (Table I). The difference between transgenic and control plants varied between 56% and 80% in the four lines analyzed ($P < 0.05$). After estimation of different yield components, reduction in seed yield was primarily due to a decrease in filling rate (the ratio of seed-filled over total florets) and, to a lesser extent, to a reduction of seed weight. The reduction in the filling rate was significant in all four transgenic lines, with an average of 67%. On the other hand, the number of panicles or the number of florets per panicle was not significantly reduced. A small, but significant reduction, in seed weight was observed in three out of the four lines analyzed (Table I).

Subsequent analysis of seeds from $T_2$ plants confirmed a drastic reduction (more than 98%) in the number of filled seeds from *KRP1*$^{OE}$ plants (Fig. 3A). Concomitantly, the total weight of filled seeds was also dramatically reduced. *KRP1* overexpression also decreased the number of seeds formed by more than 17%. Interestingly, phenotypic changes associated with Orysa;*KRP1* overexpression seemed to be ''dose dependent'' because heterozygous seeds had an intermediate phenotype for all the seed parameters analyzed (Fig. 3A). Closer inspection and sectioning of the rice *KRP1*$^{OE}$ transgenic seeds revealed that in spite of most seeds appearing morphologically normal (Fig. 3, B [right side] and C), they were in fact nearly or completely empty, whereas the maternal pericarp tissue was intact and morphologically normal. The remaining endosperm was filled with cavities (resembling a walnut structure) and no embryos were observed, either in the empty seeds or in seeds containing underdeveloped endosperm (Fig. 3D).

The nuclear DNA content of seeds from wild-type and transgenic lines was measured by flow cytometry to study the effects of Orysa;*KRP1* overexpression on the DNA ploidy distribution of the endosperm. As mentioned above, a large fraction of the seeds was empty, and so they could not be used; therefore, partially filled seeds were used instead. In overexpressing transgenic seeds, the 3C nuclei population had increased at the expense of the fraction of nuclei with 12C and 24C DNA ploidy levels (Fig. 4, A and B). Most *KRP1*$^{OE}$ seeds had undergone one round of DNA replication less, with the consequent loss of the 24C peak that was consistently present in control seeds. The total percentage of endoreduplicated nuclei decreased by almost 30% in the *KRP1*$^{OE}$ seeds (Fig. 4C), showing that KRP1 overproduction inhibits endoreduplication in the endosperm.

To analyze whether the reduction in seed production (Table I) was caused by impaired pollination,

**Table I.** *Analysis of seed production parameters from $T_1$ plants derived from KRP1*$^{OE}$ *events*

For each parameter, the average values for the transgenic siblings (TR), the average for the controls, the percentage of difference between the average for the transgenic and the average for the control plants (%Δ), and the *P* value for %Δ are listed. The different values are calculated for each of the four transgenic lines individually (008A, 013A, 004A, and 011A) and for the aggregate of the four different transgenic lines (All).

| Parameters | | Transgenic Lines | | | | |
|---|---|---|---|---|---|---|
| | | 008A | 013A | 004A | 011A | All |
| Seed yield (g) | TR | 1.1 | 1.4 | 0.7 | 2 | 1.3 |
| | control | 3.4 | 6.6 | 3.4 | 4.5 | 4.475 |
| | %Δ | −69 | −79 | −80 | −56 | −71 |
| | *P* value | 0.0119 | 0 | 0.0035 | 0.0333 | 0.0121 |
| Florets per panicle (count) | TR | 74 | 74.6 | 80.5 | 84.3 | 78.35 |
| | control | 76.9 | 81.3 | 79.8 | 79.3 | 79.325 |
| | %Δ | −4 | −8 | 1 | 6 | −1.25 |
| | *P* value | 0.8178 | 0.5326 | 0.9514 | 0.6473 | 0.7373 |
| Filling rate (%) | TR | 40.1 | 96.6 | 44.3 | 88.8 | 67.45 |
| | control | 142.1 | 308.4 | 150.8 | 199.6 | 200.225 |
| | %Δ | −72 | −69 | −71 | −56 | −67 |
| | *P* value | 0.0013 | 0.0009 | 0.0165 | 0.0216 | 0.0101 |
| Thousand seed weight (g) | TR | 22.7 | 22.2 | 20.2 | 22 | 21.775 |
| | control | 24.4 | 24.3 | 22.3 | 22.4 | 23.35 |
| | %Δ | −7 | −9 | −9 | −2 | 6.75 |
| | *P* value | 0.0256 | 0.0079 | 0.006 | 0.5057 | 0.1363 |
| Harvest index [(g/mm$^2$)E+6] | TR | 24.7 | 25.4 | 21.4 | 34.2 | 26.425 |
| | control | 74.8 | 108.7 | 52.5 | 75.8 | 77.95 |
| | %Δ | −67 | −77 | −59 | −55 | −64.5 |
| | *P* value | 0.0002 | 0 | 0.0301 | 0.0009 | 0.0078 |

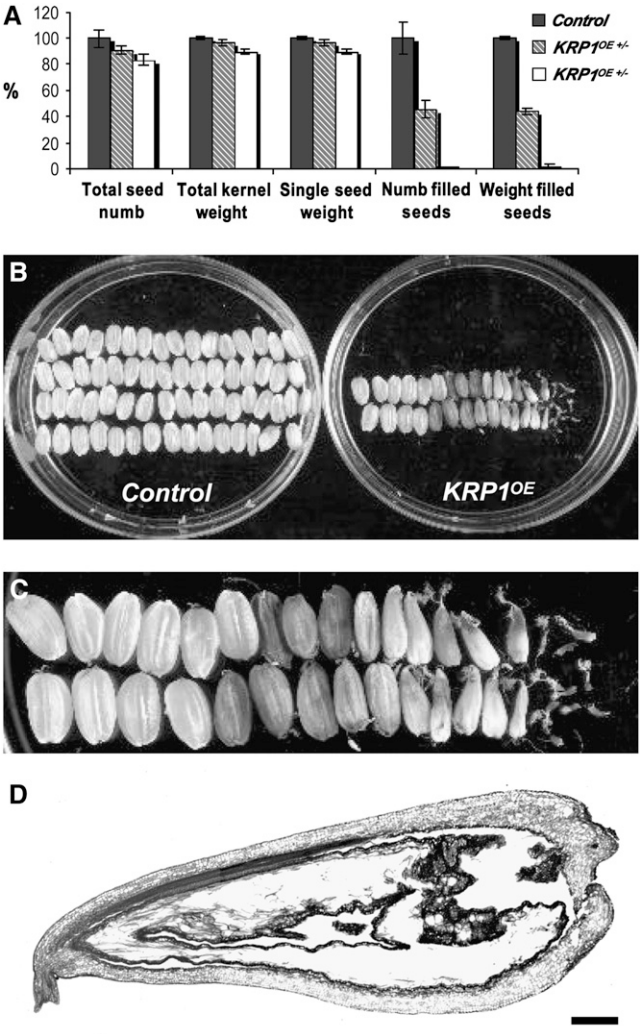


**Figure 3.** Phenotypic analysis of homozygous Orysa;*KRP1*-overexpressing seeds. A, Analysis of number and weight of filled and nonfilled seeds from *KRP1*$^{OE}$ $T_2$ plants and corresponding controls. For each parameter, the average values for the homozygous *KRP1*$^{OE}$ and control lines are shown. Bars indicate SE ($n = 10$). B, Seed populations resulting from a *KRP1*$^{OE}$ plant and corresponding control. C, Detailed image of the *KRP1*$^{OE}$ seed progeny. D, Microtome section of a *KRP1*$^{OE}$ seed showing a partially filled endosperm. Bar = 300 $\mu$m.

pollen production and viability in *KRP1*$^{OE}$ plants was investigated. The number of pollen grains per anther was approximately 5-fold lower in the homozygous transgenic plants (data not shown), and various morphological aberrations were visible in pollen of these plants (Fig. 5). The rice pollen grains stained with 4′,6-diamidino-2-phenylindole (DAPI) appeared to still comprise one vegetative and two sperm nuclei, but because their morphology was largely abnormal, it was impossible to determine precisely whether the nuclear morphology was altered in these grains. Overall pollen viability was reduced to 60%, whereas in the control plants more than 90% of the pollen grains were viable (data not shown). These data suggest that the poor seed set in *KRP1*$^{OE}$ plants was at least partly caused by reduced pollen quality.

### Tissue-Specific Accumulation of Orysa;*KRP1* Transcripts

To better understand the observed phenotypes, the expression pattern of Orysa;*KRP1* transcript levels was investigated by semiquantitative reverse transcription (RT)-PCR and real-time quantitative PCR (qPCR) in the root, shoot apex, leaf, stem, and developing seeds at different time points between 0 and 19 d after pollination (DAP). Orysa;*KRP1* was expressed in all vegetative organs (root, stem, leaf, and apex), being most abundant in leaves (Fig. 6A). In developing seeds, Orysa;*KRP1* transcripts were detected throughout seed development, but expression was highest at 8 DAP using both semiquantitative RT-PCR (data not shown) and real-time qPCR (Fig. 6B). To deduce whether the involvement of KRP1 in seed development could be common to other rice *KRP* genes, the transcript accumulation profile of the four other ones was analyzed by qPCR (Fig. 6B): *KRP1* was the only one whose expression level was low at the initial stages of seed development, peaking later at 8 DAP (as also demonstrated by RT-PCR experiments; data not shown). On the contrary, *KRP3* and *KRP5* transcripts were strongly up-regulated immediately after pollination, dropping 2 to 3 d later to basal levels. *KRP4* expression was strongly down-regulated after pollination and the abundance of *KRP2* mRNA levels was very low during seed formation, without a clear expression profile as a result. The different transcript accumulation profiles of *KRP* genes during seed development suggest a functional diversity between different KRP members.

Because both the phenotypic analysis of *KRP1*$^{OE}$ rice and the expression profile pointed toward a possible role of KRP1 in seed development, the tissue-specific accumulation pattern of Orysa;*KRP1* mRNA in developing seeds was investigated by in situ hybridization. An RNA probe for Orysa;*KRP1* was hybridized with sections of immature rice seeds, collected at 8, 10, and 15 DAP. Orysa;*KRP1* was expressed at all three stages in the pericarp and endosperm tissues (data not shown). However, a much stronger and localized signal was observed at 8 DAP in the outermost cell layers located centripetally to the endosperm (Fig. 6, C and D).

## DISCUSSION

Five *KRP* rice genes were identified with sequence similarity to other plant *KRP* genes and to the mammalian *CKI*, *p21*$^{Kip1}$. Sequence identity between the rice KRPs and those of other plants is most striking in a region of 40 amino acids located at the extreme C-terminal end of each KRP protein, which is believed to be involved in the interaction with both CYCD and CDK/CYCD complexes (Wang et al., 1998).

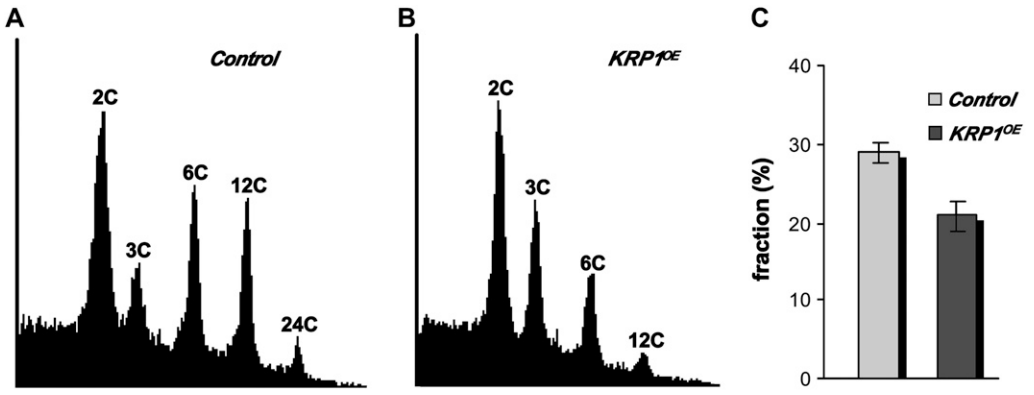


**Figure 4.** Effect of Orysa;*KRP1* overexpression on nuclear ploidy of rice endosperm. A and B, Flow cytometric analysis of nuclei from control and *KRP1*$^{OE}$ seeds, respectively. C, Percentage of endoreduplicated nuclei calculated by dividing the total number of nuclei with a ploidy equal to or greater than 12C by the total number of nuclei and multiplying by 100. Error bars denote SE ($n$ = 13).

In maize, two KRPs have recently been reported (Coelho et al., 2005) that are closely related to those of rice. Each of the maize KRPs clusters with two or three of the rice members forming two clear monocot KRP subgroups. Based on their sequences, rice KRPs group into two clades. The phylogenetic analysis suggests that monocots possess essentially two different classes of KRPs. However, it remains to be investigated experimentally whether this classification corresponds with functional differences between KRPs.

Rice plants constitutively overexpressing Orysa; *KRP1* were produced and analyzed phenotypically. A high level of expression was detected in different organs of several transgenic lines. At first sight, leaves of *KRP1*$^{OE}$ rice were only marginally shorter than those of wild-type plants. However, cell measurements revealed that mature cell length in these leaves had considerably increased. Taken together, the data indicate that overproduction of Orysa;KRP1 strongly decreased cell production and, consequently, leaf cell number. Thus, the Orysa;*KRP1* overexpression inhibits cell cycle progression, resulting in fewer but bigger cells. The existence of an organ size control mechanism that maintains organ size by regulating/compensating cell division and cell expansion has been previously described for dicot plant species and also in animals (Inzé, 2005). However, to our knowledge, such compensation mechanism is described for the first time in monocot species.

KRP overproduction has a remarkably different effect on leaf morphology in monocot versus dicot plants. Whereas the inhibition of cell division caused by the overproduction of KRPs in Arabidopsis is accompanied by a change in leaf shape (De Veylder et al., 2001), in rice *KRP*$^{OE}$ lines leaf morphology remains normal. Growth of the rice leaf results from cell proliferation at the base of the leaf and on cell elongation that takes place in the elongation zone, directly above the meristem. This spatial gradient of cell division and cell expansion results in leaf growth taking place predominantly along a one-dimensional axis. On the contrary, morphogenesis of the dicot leaf is somewhat more complex with cell division and cell elongation separated in time and space (Beemster et al., 2005). We hypothesize that because of its strictly linear organization, a decrease in cell proliferation in a rice leaf increases the length of each cell without significantly affecting leaf anatomy. On the other hand, although growth of rice and Arabidopsis leaves is very distinct both spatially and temporally, the two species are able to coregulate cell proliferation and expansion to ensure ''correct'' organ formation. Our

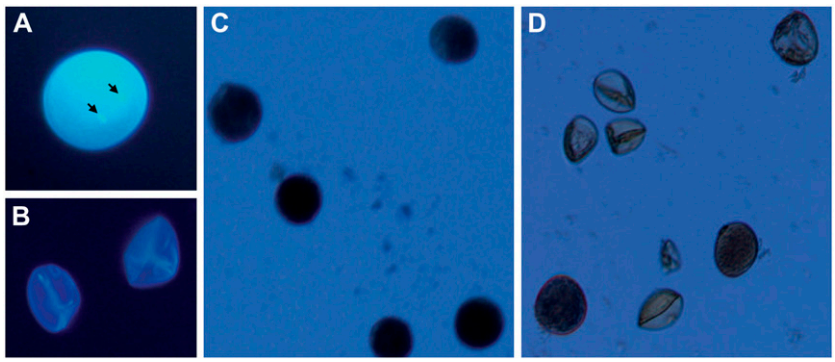


**Figure 5.** Microscopic analysis of the pollen produced by *KRP1*$^{OE}$ flowers. A and B, DAPI staining of pollen grains from a control plant showing two well-defined nuclei and of nonviable pollen grains from homozygous Orysa;*KRP1*-overexpressing plant, respectively. C and D, Mature pollen grains from control plants and from homozygous *KRP1*$^{OE}$ plants, respectively.

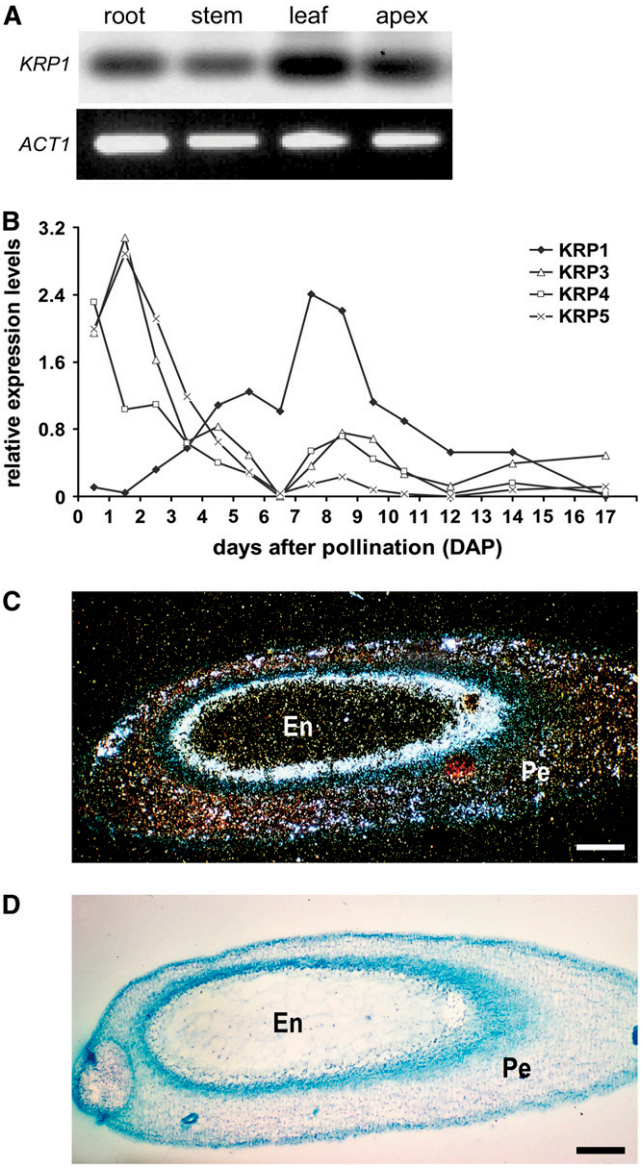


**Figure 6.** Rice *KRP* transcript accumulation. A, Expression profiles of Orysa;*KRP1* (*KRP1*) transcript in rice tissues whose levels were measured in roots, stems, leaves, and shoot apical meristems by semiquantitative RT-PCR. cDNA prepared from the indicated tissues were subjected to semiquantitative RT-PCR analysis with gene-specific primers (see "Materials and Methods"). B, Expression analysis of rice *KRP1*, *KRP3*, *KRP4*, and *KRP5* during seed development, as determined by qPCR analysis. cDNA prepared from developing seeds were subjected to qPCR analysis using gene-specific primers (see "Materials and Methods"). The rice *actin1* gene (*ACT1*) was used as a loading control (A and B). The values represent expression fold change compared to the time point with lowest transcript level. C and D, Expression pattern of Orysa;*KRP1* in developing rice seeds as revealed by in situ hybridization, using dark-field and bright-field optics, respectively. Both micrographs show longitudinal sections of rice caryopsis at 8 DAP. En, Endosperm; Pe, pericarp. Bar = 250 $\mu$m.

results suggest that a compensatory mechanism is probably active and important for the maintenance of plant growth, independent of the developmental peculiarities between species.

Orysa;*KRP1* overexpression in rice plants reduces seed yield by approximately 70%, mainly caused by a drop in the seed-filling rate and, to a small extent, by a decrease in the average seed weight, which might be the consequence of a disturbance in cell expansion and/or cell division during endosperm formation. A role for Orysa;*KRP1* in endosperm formation is also inferred from its expression profile during seed development. In developing seeds harvested during the first 19 DAP, the expression of endogenous Orysa;*KRP1* was highest at 8 DAP. Cell division in the rice endosperm and embryo is completed approximately 9 to 10 DAP (Hoshikawa, 1993), suggesting that Orysa;KRP1 is probably involved in controlling the exit from the mitotic cell cycle. The other rice *KRP* genes were mostly expressed 0 to 4 DAP, hinting at alternative roles in seed formation. In accordance, overexpression of Orysa;*KRP4* belonging to the second clade of monocot *KRP* genes had no effect on seed production (data not shown), excluding that the *KRP1*$^{OE}$ phenotype observed and the deduced function of *KRP1* in seed development could be common to all rice *KRP* genes.

Rice endosperm begins as a triploid tissue resulting from the union of two polar nuclei and one sperm nucleus. After fertilization, endosperm growth is the result of increases in both cell number and cell size. For the first days after pollination, the endosperm nuclei divide synchronously without cell wall formation. At 4 DAP, the endosperm nuclei near the embryo begin to form cell walls, enclosing the nucleus and protoplasma. The endosperm changes from a multinucleate, single-cell to a uninucleate, multicellular structure, after which all multiplication takes place only by cell division. During this period, cell multiplication in the endosperm is confined mainly to the outermost peripheral cell layer. Newly formed cells are added centripetally so that the dividing cell layer remains at the periphery (Hoshikawa, 1993). Coincidentally, we found by in situ mRNA hybridization that Orysa;*KRP1* is mostly expressed 8 h after pollination in the cell layers along the periphery of the developing endosperm. This region corresponds to the cell layers that have been most recently generated through cellular division and will soon thereafter halt division (9–10 DAP). Interestingly, sectioning of the *KRP1*$^{OE}$ seeds showed that the outermost endosperm cell layers occupy a large part of the endosperm space, making a number of cavities, whereas the most inner layers are nearly absent, indicating that KRP overproduction impairs the production of a sufficient number of cell layers.

Endosperm cell division ends 9 to 10 DAP, and the total number of cells is determined. As the number of mitotic divisions decreases, the average DNA content per nucleus rapidly increases because of endoreduplication. From the Orysa;*KRP1* transcript accumulation

profile, this inhibitor can be inferred to be implicated in both cell proliferation and endoreduplication, given that expression could be detected throughout seed formation. However, both the in situ hybridization and semiquantitative expression analysis showed that Orysa;*KRP1* expression reaches its maximum when cell proliferation ends and endoreduplication starts, indicating that Orysa;KRP1 at endogenic levels plays an important role in the switch from mitosis to endocycle.

Endoreduplication has a central function in endosperm formation (Larkins et al., 2001). To analyze whether the effects observed in seeds after Orysa; *KRP1* overexpression could be related with the endosperm DNA ploidy distribution, the DNA content of seeds from wild-type and transgenic lines was measured by flow cytometry. In $KRP1^{OE}$ lines, the 3C nuclei population increased, in correlation with a decrease in the number of nuclei with a 12C and 24C ploidy level. This inhibition of the endoreduplication cycle is in agreement with previous reports on strong *KRP* overexpression in Arabidopsis and tobacco (De Veylder et al., 2001; Jasinski et al., 2002; Zhou et al., 2002b; Schnittger et al., 2003). However, to our knowledge, no effects on seed size or seed yield have been previously reported in other plant species overproducing or down-regulating KRPs.

The reduced seed production observed in rice overexpressing Orysa;*KRP1* is probably related to the low pollen quality. Previously, plants overexpressing *AtKRP1* under control of the *Bgp1* promoter of *Brassica campestris* were shown to produce a reduced amount of seeds because of the inability of the formed pollen grains to germinate. All together, these data indicate that KRP1 might play a critical role in pollen development. However, because the transgenic pollen grains stained with DAPI were largely abnormal, we could not statistically determine whether nuclear morphology and nucleus number could be altered in these grains. Recently, a pollen phenotype has been described resulting from mutation of the CDKA;1 protein in Arabidopsis (Nowack et al., 2006). The *cdka;1* mutant pollen failed to undergo the second meiosis, resulting in pollen grains with only one nucleus instead of two. This defect, though, did not generally change pollen morphology, or affect viability or germination ability. On the contrary, *KRP1* overexpression results in abnormally shaped pollen grains and affects viability and/or ability to germinate, as deduced from the reduced number of formed seeds. This evidence points to a role for Orysa;*KRP1* in pollen formation distinct from that for *CDKA;1*; however, we cannot exclude that KRP1 is implicated in meiosis and somehow cross talks with CDKA;1 during the development of the male gametocytes.

Arrest in pollen development has also been found associated with loss of SCF function in Arabidopsis (Wang and Yang, 2005). SCF complexes are ubiquitin protein ligases with several subunits, e.g. SKP1, Cul1, F-box proteins, and Ring-H2 finger protein (Rbx1). Analysis of a mutant version of one Arabidopsis *SKP1* gene, *ASK1*, has unraveled the role of this gene in the meiotic process that gives rise to the male gametophytes (Wang and Yang, 2005). Also, the *Cul1* gene has been shown to be essential for embryo proliferation, demonstrating the importance of SCF proteolysis in seed formation (Shen et al., 2002). Another subunit of the SCF complex, Rbx1, is preferentially active in proliferating tissues, suggesting a role in the turnover of cell cycle regulators (Lechner et al., 2002). In mammalian cells, SCF complexes are important in controlling cell cycle through ubiquitin-mediated proteolysis of G1-to-S regulators, including ICKs (for review, see Nakayama and Nakayama, 2005). In plants, the importance of SCF complexes in the regulation of KRPs remains to be conclusively demonstrated, even if some evidence points toward some plant KRPs as being regulated through proteolysis (for review, see Verkest et al., 2005b). All together, rice *KRP1* overexpression might interfere with the developmentally regulated degradation of KRP1 by SCF, resulting in abnormal pollen and embryo development. However, presently there is no experimental evidence to rule out alternative models. For example, it remains to be investigated whether the observed endosperm defects could reflect the involvement of rice KRP1 in programmed cell death as previously demonstrated for the Arabidopsis ICK1/KRP1 (Schnittger et al., 2003). Unfortunately, loss-of-function alleles or insertional mutants, which would be invaluable to challenge these hypotheses and help us to clarify the underlying mechanisms that govern rice KRP1 regulation, are currently not available.

In summary, our data point to a critical role for Orysa;*KRP1* in vegetative and reproductive developmental processes, including pollen development, seed formation, and leaf cell division/expansion. Artificial modulation of *KRP* expression levels during seed development could provide feasible approaches for increasing seed yield in plants. The possible role of Orysa;*KRP1* in endosperm development should be carefully elucidated given that the endosperm constitutes the largest part of the rice seed; clarifying the cellular and molecular events that contribute to normal endosperm development might provide a better understanding of the components of seed production and offer the possibility to engineer grain yield.

## MATERIALS AND METHODS

### Construction of a Rice cDNA Library

Total RNA was extracted from rice (*Oryza sativa*) cell suspension cultures harvested at 0, 3, 6, 9, and 12 d after subculture in fresh medium. Equimolar amounts (100 $\mu$g) of total RNA from each sample were used to purify poly($A^+$) mRNA with the Poly(A) Quick mRNA Isolation kit (Stratagene). The synthesis and subcloning of the cDNA into the HybriZAP-2.1 $\lambda$ vector were performed according to the manufacturer's instructions (Stratagene). Approximately $2 \times 10^6$ independent plaque-forming units were produced, with an average insert size of 1 kb. The library was amplified once to yield $2 \times 10^9$ plaque-forming units $mL^{-1}$.

## Identification of Rice KRPs and Cloning of the Orysa;*KRP1*

In an attempt to identify rice *KRP* genes, public sequence databases were screened for the KYNFD and GRYEW amino acid motifs located at the C-terminal end of most plant KRPs (De Veylder et al., 2001), using the BLAST program. Primers (5′-CCGCCGAGATCGAGGCGTTCTTCG-3′ and 5′-AAACCTCTGATAAATACTGGGACG-3′) were designed to amplify by PCR a 430-bp sequence of an identified rice Orysa;*KRP1* expressed sequence tag (accession no. AU075786), using a plasmid preparation from a cDNA library as template. The amplified fragment was cloned into the pUC18 vector and sequenced for sequence confirmation.

To clone the full-length Orysa;*KRP1* cDNA, approximately 750,000 plaque-forming units from the rice cell suspension cDNA library were screened by hybridization with the PCR-amplified expressed sequence tag fragment as a probe (Terras et al., 1995). Five positive plaques could be identified for Orysa;*KRP1*. After purification, the DNA of the positive phages was excised; the inserts were cloned into the pAD-GAL4-2.1 vector and sequenced.

## Sequence Analysis and Phylogeny

Based on the sequence of Orysa;*KRP1*, four other *KRP* genes could be identified for rice from The Institute for Genome Research (TIGR pseudomolecule assembly release 3). Protein sequences were aligned with ClustalW (Thompson et al., 1994). The alignments were edited and reformatted with BioEdit (http://www.mbio.ncsu.edu/BioEdit/bioedit.html). Similarity between protein sequences was based on a BLOSUM62 matrix. Phylogenetic analysis was performed on the conserved C-terminal region. A phylogenetic tree was constructed with the neighbor-joining algorithm of the software package TREECON (Van de Peer and De Wachter, 1994).

## Generation of Rice *KRP1*$^{OE}$ Transgenic Lines and Growth Conditions

The pDONR-*KRP1* entry clone was used to transfer the Orysa;*KRP1* cDNA into a Gateway-compatible plant transformation binary vector containing a hygromycin phosphotransferase (*HPT*)-based selectable marker cassette and a green fluorescent protein-based visual marker cassette. The Orysa;*KRP1* cDNA was linked at its 5′ end to the *GOS2* promoter (de Pater et al., 1992) and at its 3′ end to the *ZEIN* terminator (Wu et al., 1993).

Rice cv Nipponbare was transformed according to Hervé and Kayano (2006). Hardened plantlets were grown in the greenhouse under 60% to 70% relative humidity, 550 $\mu$mol $m^{-2}$ $s^{-1}$ photosynthetically active radiation of supplementary artificial lighting with sodium pressure lamps, a temperature regime of 28°C day/22°C night, with a 11.5-h daylength.

For copy number estimation, genomic DNA was isolated from small segments of mature leaves from transgenic lines ($T_1$) using the Wizard Magnetic 96 DNA kit (Promega) and subjected to qPCR using Taqman probes in multiplex qPCR (Ingham et al., 2001; Yang et al., 2005). Both the endogenous single-copy rice *GOS5* gene, used as internal control, and the *HPT* transgene were amplified in a single tube reaction. The following oligonucleotides were used: 5′-CGCTGCGGCCGATCT-3′ (forward primer), 5′-CCATGTAGTGTATTGACCGATTCCT-3′ (reverse primer), and 5′-Fam-ACGAGCGGGTTCGGCCCATTC-Tamra-3′ (Taqman probe) for *HPT*, and 5′- TACGGCGAGAAGAGCGTCTACT-3′ (forward primer), 5′-CGAACGTC-TCGAAGAACTTGCT-3′ (reverse primer), and 5′-Vic-CCTCGAGGACATC-GGCAACACCA-Tamra-3′ (Taqman probe) for *GOS5*. The real-time PCR reactions were carried out with the 7900 HT sequence detection system (Applied Biosystems) in 384-well reaction plates. For determination of the copy number of the selection marker gene, a standard curve was established with a serial dilution of genomic DNA extracted from a single-copy transgenic rice plant. For every sample, the number of molecules for the *GOS5* and *HPT* genes were calculated against their standard curves. Only transgenic events containing a single transgene insert were retained.

## Phenotypic Evaluation of *KRP1*$^{OE}$ Plants

Fifteen independent $T_0$ transgenic plants, containing the Orysa;*KRP1* coding sequence under the control of the rice constitutive *GOS2* promoter, were regenerated in vitro and transferred to soil. Four transformation events containing a single copy of the transgene, as determined by real-time qPCR (Ingham et al., 2001; Yang et al., 2005), were selected for further analysis based on the existence of a phenotype. Orysa;*KRP1* transcript levels were determined in two to three $T_1$ plants for each $T_0$ event; the $T_1$ plants were confirmed to contain the transgene by PCR analysis (see below) and green fluorescent protein detection (see Supplemental Methods S1). $T_1$ plants lacking the transgene due to segregation were used as controls for each line. After selection, seedlings were transplanted in 0.5-L pots filled with clay-rich potting soil. Greenhouse conditions were as above.

From transplantation until maturity, each plant was digitally imaged. Image analysis software was used for the calculation of several growth parameters (for more details, see Supplemental Methods S1). When the plants had reached maturity, the primary panicles were counted, harvested, and threshed (separation of seeds from vegetative part). The unfilled and filled (rice grain-containing) florets were taken apart, independently counted, and weighed (for more details, see Supplemental Methods S1). Through this procedure, the following seed-related parameters were obtained: seed yield (weight of filled florets per plant in grams); panicle number; florets per panicle; filling rate (%); 1,000 seed weight (g); and harvest index, i.e. ratio between seed yield per plant (g) and the aboveground plant area ($mm^2$), multiplied by a $10^6$ factor.

All parameters were analyzed by two-factor ANOVA for transgenic state (populations with and without the transgene) and event differences. If $P$ (transgenic state) $< 0.05$, an overall ''transgene'' effect was considered causing the differences in phenotype. To check for an effect of the transgene within an event, i.e. for detecting line-specific effects, a pair-wise comparison $t$ test based on the ANOVA results, using $P < 0.05$ as a cutoff, was performed for each event, between the transgenic plants and their corresponding control siblings. Flow cytometric analysis was performed with a CyFlow (Partec) as described (Boudolf et al., 2004).

## Measurement of LERs

Leaf elongation rates were determined by measuring leaf length twice a day and calculating growth in function of time. Homozygous transgenic and control plants were grown in parallel and the length of the sixth leaf was measured by ruler as the distance from its tip to the soil surface. This measurement was carried out on at least 15 plants each time from leaf emergence to complete extension. LER of individual leaves was calculated as the slope of the regression fitted through the data points. A local polynomial fit of third degree on five data points was used to estimate the slope of the midpoint. For the first and last two points, the slope was determined on the first and last five points of the dataset, respectively.

## Determination of Mature Cell Length and Cell Production Rates

Segments of the fully mature region of sixth leaves were collected, placed in methanol for chlorophyll removal and fixation for at least 2 d, and transferred in 90% (w/v) lactic acid (Merck) for clearing, storage, and mounting on microscopy slides. Cells were measured using image analysis on differential interphase contrast images. The setup consisted of a light microscope (Axioskop; Zeiss) equipped with a monochrome CCD camera 4912 (Cohu Electronics). The image was acquired by a computer equipped with Scion Image program (http://www.scioncorp.com). The lengths of individual cells were measured with the image analysis program ImageJ (publicly available on http://rsb.info.nih.gov/ij/) by tracing straight lines between successive transverse cell walls. The values obtained were averaged between different leaves and used to compare transgenic and control plants. The rate of cell production (cells $h^{-1}$) per cell file in the meristem was calculated as the ratio between the LER (mm $h^{-1}$) and the length (mm) of the mature cells (Fiorani et al., 2000).

## Determination of Pollen Number per Anther and Pollen Viability

Anthers were collected from flowers immediately after anthesis and gently squashed in a droplet of water; the number of grains released was counted under the microscope. To analyze the viability, the collected pollen grains were fixed in ethanol:acetic acid (3:1), dehydrated through ethanol series, and stored in 70% ethanol. Before analysis, anthers were rehydrated in 1× phosphate buffered saline. Morphological integrity of the pollen grains was analyzed by staining them with 1% (w/v) iodine-potassium iodide (Khatun and Flowers, 1995). Pollen viability was assessed by staining with

1 $\mu$g/mL DAPI in 1× phosphate buffered saline to detect the presence of the two generative nuclei. The pollen was considered viable and morphologically normal when the two generative nuclei were clearly visible and when the pollen wall was intact and the content evenly stained, respectively.

## Orysa;*KRP1* Expression in Wild-Type and Transgenic Lines

Total RNA was extracted from 10-d-old seedling organs (roots, leaves, stems, and apex) or immature seeds harvested daily between 0 and 11, and at 13, 15, and 19 DAP from greenhouse-grown plants. For semiquantitative RT-PCR, 2 $\mu$g of each sample was reverse transcribed into cDNA with the SuperScript First-Strand Synthesis System for RT-PCR (Invitrogen). PCR amplification of the Orysa;*KRP1* cDNA was carried out with the following gene-specific primers: 5′-CCGCCGAGATCGAGGCGTTCTTCG-3′ and 5′- AAACCTCTGATAAATACTGGGACG-3′ (forward and reverse, respectively). The PCR products were separated on a 1% (w/v) agarose gel and transferred to a nylon membrane (Hybond N; GE-Biosciences) by blotting. Hybridizations were performed with the same probe used for the cDNA library screening and labeled with the North2South Biotin Random Prime kit (Pierce). Detection was done with the North2South Chemiluminescent Nucleic Acid Hybridization and Detection kit (Pierce), according to the manufacturer's protocol.

Real-time qPCR was performed on cDNA prepared from total RNA using the Taqman Reverse Transcription Reagents kit (Applied Biosystems) according to the manufacturer's instructions. Total RNA was extracted from 10-mg tissue samples with the Nucleic Acid Purification System 6100 (Applied Biosystems) and the ABI Prism 6100 Nucleic Acid PrepStation (Applied Biosystems). The multiplex PCR reactions were carried out in 384-well plates with Taqman probes and the ABI Prism 7900 HT sequence detection system. Specific primers and probes were used: 5′-CCGCGAGAGGAGAGAAACAA-3′ (forward primer), 5′-TGCTGTGCTGAGGCTGTTG-3′ (reverse primer), and 5′-Fam-CAGATCGCTCACCTCGCCGGG-Tamra-3′ (Taqman probe) for Orysa;*KRP1* transcripts, and 5′-CGCCGGTCGGTTCGA-3′ (forward primer), 5′-GACACTGCCACCCATGGT-3′ (reverse primer), and 5′-Vic-ATGCGTGACACATTATT-Tamra-3′ (Taqman probe) for the 18S rRNAs, which were used as an internal control. For transcript quantification by qPCR of the additional *KRP* genes of rice, the following primer pairs were used: ATTGTTGGGCTGTTCTGGTGAG (forward) and TGCTGCTTGGCCTCCTGG (reverse) for *KRP2*; AGCACAAGCACAACCCTGC (forward) and GGGCAATGTCGTAATTGTACTTCTC (reverse) for *KRP3*; AGAGCTGGAAGCGTTCTTCG (forward) and GGCAGTCATTCACAGGATCAAAG (reverse) for *KRP4*; and CCCCTGGCTCCACAACTAAAAC (forward) and CCATCTCAAGAGAACTCGGAACG (reverse) for *KRP5*. cDNA was amplified for multiplex PCR with TaqMan Universal PCR Master Mix (Applied Biosystems), according to the manufacturer's instructions. All multiplex PCR reactions were performed in duplicate. The cycle values at which the crossing point between the amplification curve and the threshold occurred were defined as the threshold cycle (Ct values). To determine the expression level of Orysa;*KRP1*, the comparative $\Delta\Delta$Ct method was used. The normalization against 18S rRNA internal control was done by subtracting the average Orysa;*KRP1* Ct values from the average 18S Ct values ($\Delta$Ct). By comparing the $\Delta$Ct values of the transgenic samples to the $\Delta$Ct values of a nontransgenic sample, the $\Delta\Delta$Ct values were obtained. The fold changes of gene expression between two samples were calculated by using the $\Delta\Delta$Ct in the formula: fold change = $2^{\Delta\Delta Ct}$.

## Analysis of Orysa;*KRP1* Tissue Accumulation by in Situ Hybridization

The in situ hybridization of sections through developing rice seeds was performed according to de Almeida-Engler et al. (2001). The full-length Orysa;*KRP1* cDNA was cloned in pSP18 and pSP19 plasmids in sense and antisense orientation and the purified, linearized plasmids were used to generate the riboprobes by in vitro transcription according to the manufacturer's instructions (Promega).

The accession numbers for the sequences referred to in the article are: AAC49698 (AtKRP1), CAB76424 (AtKRP2), CAC41617 (AtKRP3), CAC41618 (AtKRP4), CAC41619 (AtKRP5), CAC41620 (AtKRP6), CAC41621 (AtKRP7), CAA05215 (CrKRP), AAV76001 (EeKRP), AI728644 (GhKRP1), AAS13376 (GmKRP2;1), AAS13374 (GmKRP1;1), AAS13375 (GmKRP1;2), AAS13377 (GmKRP2;2), CAD29648 (LeKRP1), CAD29649 (LeKRP2), AJ297905 (NsKIS1a), CAD56868 (NtaKIS2), CAC82733 (NtoKIS1a), BAB20860 (PsKRP), AAX85449 (ZmKRP1), and AAX85450 (ZmKRP2).

## Supplemental Data

**Supplemental Methods S1.** Phenotypic evaluation of $KRP1^{OE}$ plants.

**Supplemental Figure S1.** Expression levels of Orysa;*KRP1* in the transgenic plants as determined by real-time qPCR.

**Supplemental Table S1.** Analysis of vegetative growth parameters of $T_1$ generation plants derived from $KRP1^{OE}$ events.

## ACKNOWLEDGMENTS

We thank the members of the leaf growth and development group for critical reading of the manuscript and Martine De Cock for help in preparing it.

Received July 20, 2006; accepted September 21, 2006; published September 29, 2006.

## LITERATURE CITED

**Beemster GTS, De Veylder L, Vercruysse S, West G, Rombaut D, Van Hummelen P, Galichet A, Gruissem W, Inzé D, Vuylsteke M** (2005) Genome-wide analysis of gene expression profiles associated with cell cycle transitions in growing organs of Arabidopsis. Plant Physiol **138:** 734–743

**Bisbis B, Delmas F, Joubès J, Sicard A, Hernould M, Inzé D, Mouras A, Chevalier C** (2006) Cyclin-dependent kinase (CDK) inhibitors regulate the CDK-cyclin complex activities in endoreduplicating cells of developing tomato fruit. J Biol Chem **281:** 7374–7383

**Boudolf V, Vlieghe K, Beemster GTS, Magyar Z, Torres Acosta JA, Maes S, Van Der Schueren E, Inzé D, De Veylder L** (2004) The plant-specific cyclin-dependent kinase CDKB1;1 and transcription factor E2Fa-DPa control the balance of mitotically dividing and endoreduplicating cells in Arabidopsis. Plant Cell **16:** 2683–2692

**Coelho CM, Dante RA, Sabelli PA, Sun Y, Dilkes BP, Gordon-Kamm WJ, Larkins BA** (2005) Cyclin-dependent kinase inhibitors in maize endosperm and their potential role in endoreduplication. Plant Physiol **138:** 2323–2336

**de Almeida Engler J, De Groodt R, Van Montagu M, Engler G** (2001) *In situ* hybridization to mRNA of *Arabidopsis* tissue sections. Methods **23:** 325–334

**de Pater BS, van der Mark F, Rueb S, Katagiri F, Chua N-H, Schilperoort RA, Hensgens LAM** (1992) The promoter of the rice gene *GOS2* is active in various different monocot tissues and binds rice nuclear factor ASF-1. Plant J **2:** 837–844

**De Veylder L, Beeckman T, Beemster GTS, Krols L, Terras F, Landrieu I, Van Der Schueren E, Maes S, Naudts M, Inzé D** (2001) Functional analysis of cyclin-dependent kinase inhibitors of Arabidopsis. Plant Cell **13:** 1653–1667

**De Veylder L, Joubès J, Inzé D** (2003) Plant cell cycle transitions. Curr Opin Plant Biol **6:** 536–543

**Dewitte W, Murray JAH** (2003) The plant cell cycle. Annu Rev Plant Biol **54:** 235–264

**Fiorani F, Beemster GTS, Bultynck L, Lambers H** (2000) Can meristematic activity determine variation in leaf size and elongation rate among four *Poa* species? A kinematic study. Plant Physiol **124:** 845–855

**Hervé P, Kayano T** (2006) Japonica rice varieties (*Oryza sativa*, Nipponbare, and others). *In* K Wang, ed, *Agrobacterium* Protocols, Vol 1, Ed 2. Humana Press, Totowa, NJ, pp 213–222

**Himanen K, Boucheron E, Vanneste S, de Almeida Engler J, Inzé D, Beeckman T** (2002) Auxin-mediated cell cycle activation during early lateral root initiation. Plant Cell **14:** 2339–2351

**Hoshikawa K** (1993) Anthesis, fertilization and development of caryopsis. *In* T Matsuo, K Hoshikawa, eds, Science of the Rice Plant, Vol 1: Morphology. Food and Agriculture Policy Research Center, Tokyo, pp 339–376

**Ingham DJ, Beer S, Money S, Hansen G** (2001) Quantitative real-time PCR assay for determining transgene copy number in transformed plants. Biotechniques **31:** 132–140

**Inzé D** (2005) Green light for the cell cycle. EMBO J **24:** 657–662

**Jasinski S, Perennes C, Bergounioux C, Glab N** (2002) Comparative molecular and functional analyses of the tobacco cyclin-dependent kinase inhibitor NtKIS1a and its spliced variant NtKIS1b. Plant Physiol **130:** 1871–1882

**Khatun S, Flowers TJ** (1995) The estimation of pollen viability in rice. J Exp Bot **46:** 151–154

**Larkins BA, Dilkes BP, Dante RA, Coelho CM, Woo Y-m, Liu Y** (2001) Investigating the hows and whys of DNA endoreduplication. J Exp Bot **52:** 183–192

**Lechner E, Xie D, Grava S, Pigaglio E, Planchais S, Murray JA, Parmentier Y, Mutterer J, Dubreucq B, Shen WH, et al** (2002) The AtRbx1 protein is part of plant SCF complexes, and its down regulation causes severe growth and developmental defects. J Biol Chem **277:** 50069–50080

**Lui H, Wang H, DeLong C, Fowke LC, Crosby WL, Fobert PR** (2000) The *Arabidopsis* Cdc2a-interacting protein ICK2 is structurally related to ICK1 and is a potent inhibitor of cyclin-dependent kinase activity *in vitro*. Plant J **21:** 379–385

**Nakayama KI, Nakayama K** (2005) Regulation of the cell cycle by SCF-type ubiquitin ligases. Semin Cell Dev Biol **16:** 323–333

**Nowack MK, Grini PE, Jakoby MJ, Lafos M, Koncz C, Schnittger A** (2006) A positive signal from the fertilization of the egg cell sets off endosperm proliferation in angiosperm embryogenesis. Nat Genet **38:** 63–67

**Schnittger A, Weinl C, Bouyer D, Schöbinger U, Hülskamp M** (2003) Misexpression of the cyclin-dependent kinase inhibitor *ICK1/KRP1* in single-celled Arabidopsis trichomes reduces endoreduplication and cell size and induces cell death. Plant Cell **15:** 303–315

**Shen WH, Parmentier Y, Hellmann H, Lechner E, Dong A, Masson J, Granier F, Lepiniec L, Estelle M, Genschik P** (2002) Null mutation of AtCUL1 causes arrest in early embryogenesis in Arabidopsis. Mol Biol Cell **13:** 1916–1928

**Sherr CJ, Roberts JM** (1995) Inhibitors of mammalian $G_1$ cyclin-dependent kinases. Genes Dev **9:** 1149–1163

**Sherr CJ, Roberts JM** (1999) CDK inhibitors: positive and negative regulators of $G_1$-phase progression. Genes Dev **13:** 1501–1512

**Terras FRG, Eggermont K, Kovaleva V, Raikhel NV, Osborn RW, Kester A, Rees SB, Torrekens S, Van Leuven F, Vanderleyden J, et al** (1995) Small cysteine-rich antifungal proteins from radish: their role in host defense. Plant Cell **7:** 573–588

**Thompson JD, Higgins DG, Gibson TJ** (1994) CLUSTAL W: improving the sensitivity of progressive multiple sequence alignment through sequence weighting, position-specific gap penalties and weight matrix choice. Nucleic Acids Res **22:** 4673–4680

**Van de Peer Y, De Wachter R** (1994) TREECON for Windows: a software package for the construction and drawing of evolutionary trees for the Microsoft Windows environment. Comput Appl Biosci **10:** 569–570

**Verkest A, de O Manes C-L, Maes S, Van Der Schueren E, Beeckman T, Genschik P, Inzé D, De Veylder L** (2005a) The cyclin-dependent kinase inhibitor KRP2 controls the onset of the endoreduplication cycle during Arabidopsis leaf development through inhibition of mitotic CDKA;1 kinase complexes. Plant Cell **17:** 1723–1736

**Verkest A, Weinl C, Inzé D, De Veylder L, Schnittger A** (2005b) Switching the cell cycle. Kip-related proteins in plant cell cycle control. Plant Physiol **139:** 1099–1106

**Wang H, Fowke LC, Crosby WL** (1997) A plant cyclin-dependent kinase inhibitor gene. Nature **386:** 451–452

**Wang H, Qi Q, Schorr P, Cutler AJ, Crosby WL, Fowke LC** (1998) ICK1, a cyclin-dependent protein kinase inhibitor from *Arabidopsis thaliana* interacts with both Cdc2a and CycD3, and its expression is induced by abscisic acid. Plant J **15:** 501–510

**Wang H, Zhou Y, Gilmer S, Whitwill S, Fowke LC** (2000) Expression of the plant cyclin-dependent kinase inhibitor ICK1 affects cell division, plant growth and morphology. Plant J **24:** 613–623

**Wang Y, Yang M** (2005) The ARABIDOPSIS SKP1-LIKE1 (ASK1) protein acts predominately from leptotene to pachytene and represses homologous recombination in male meiosis. Planta **9:** 1–5

**Weinl C, Marquardt S, Kuijt SJH, Nowack MK, Jakoby MJ, Hülskamp M, Schnittger A** (2005) Novel functions of plant cyclin-dependent kinase inhibitors, ICK1/KRP1, can act non-cell-autonomously and inhibit entry into mitosis. Plant Cell **17:** 1704–1722

**Wu L, Ueda T, Messing J** (1993) 3′-end processing of the maize 27 kDa zein mRNA. Plant J **4:** 535–544

**Yang L, Ding J, Zhang C, Jia J, Weng H, Liu W, Zhang D** (2005) Estimating the copy number of transgenes in transformed rice by real-time quantitative PCR. Plant Cell Rep **23:** 759–763

**Zhou Y, Fowke LC, Wang H** (2002a) Plant CDK inhibitors: studies of interactions with cell cycle regulators in the yeast two-hybrid system and functional comparisons in transgenic *Arabidopsis* plants. Plant Cell Rep **20:** 967–975

**Zhou Y, Wang H, Gilmer S, Whitwill S, Fowke LC** (2002b) Effects of co-expressing the plant CDK inhibitor ICK1 and D-type cyclin genes on plant growth, cell size and ploidy in *Arabidopsis thaliana*. Planta **216:** 604–613